Journal of Molecular Graphics and Modelling 91 (2019) 1–9

Contents lists available at ScienceDirect

Journal of Molecular Graphics and Modelling

journal homepage: www.elsevier.com/locate/JMGM

# New modeling method to simulate asphaltenes at oil sands process in water management

Jing Yuan [a, b, c, *], Lexuan Zhong [c], Mohammadtaghi Vakili [a], Giwa Abdulmoseen Segun [a]

[a] Green Intelligence Environment School, Yangtze Normal University, China
[b] CanmetENERGY Devon Research Centre, Natural Resources Canada, 1 Oil Patch Drive, Devon, Alberta, T9G 1A8, Canada
[c] University of Alberta, 9211-116 Street NW, T6G 1H9, Canada

ARTICLE INFO

*Article history:*
Received 20 March 2019
Received in revised form
15 May 2019
Accepted 16 May 2019
Available online 17 May 2019

*Keywords:*
Molecular dynamic (MD) simulation
Asphaltene's aggregation
Dynamics properties
Water-oil interfaces

ABSTRACT

The study of various structures, physicochemical structures and dynamic characteristics of oil-water interface asphaltenes is an important basis for the large-scale development and efficient clean utilization of oil sands. The molecular dynamics simulations method provides a possibility for revealing the physicochemical structure and dynamic characteristics of oil sands. The emphasis of this paper is to study the physic-chemical structure of tar sands asphaltenes and the changes of their kinetic properties by using molecular dynamics simulations. Molecular dynamics was used to simulate the physicochemical and dynamic characteristics of asphaltenes in water treatment of the oil sands. In this research, the structural and dynamic properties of asphaltenes, such as density distribution, correlation (radial distribution function), root-mean-square deviation (RMSD), and mean azimuth shift (MSD), diffusion coefficient, the radius of gyration, volume viscosity and free energy in water treatment were systematically discussed. The simulation results of asphaltene at the oil-water interface revealed that, in the oil-water interface, oil and water will affect the solubility of asphaltene. The asphaltene molecules have different mobility and the ability to break molecular association, indicating that the structure and dynamic properties of asphaltene in the oil-water interface and the water-water interface are different.



## 1. Introduction

The influence of asphaltenes on the production, transportation, refining and utilization of petroleum [1] makes it more urgent to study the various structures, physicochemical structures and dynamic characteristics of oil-water interface asphaltenes. In the process of organic matter producing oil and water and transportation, water and oil are produced together, and thus exposed to enough mixed energy to form the dispersion of water droplets in oil [2]. On the contrary, at the water-oil interface, water droplets disperse in water. In addition, petroleum production and transportation processes contain many interfacial active components, namely, asphaltenes, resins and naphthenic acids [3–5]. These components may accumulate at the oil-water interface, preventing the droplets from reforming into a single phase. Among these components, asphaltenes are considered as the main material for emulsion stability, because asphaltenes are easy to adsorb in the water interface of crude oil or other water solvents, thus forming a rigid film around water droplets [6], thus protecting the interface membrane from cracking when water droplets collide [7–10]. At present in view of the oil-water interface of various structure, physical and chemical structure and dynamics of the asphaltenes features a lot of methods are used in research work, such as Yahya H.K hraisha [11] the pyrolysis of pitch extraction was studied for the Jordan oil sands, under nitrogen atmosphere to TG thermal analysis after extraction of the asphalt, and the total package first order reaction model to solve the kinetic parameters; Young Cheol Park [12] conducted TG pyrolysis analysis on Alberta's oil sands, extracted the asphalt and made various measurements accordingly, and finally calculated the kinetic parameters with the first-order reaction model of the total package. Pulikesi Muruganet al. [13] studied the exothermic peak of low-temperature oxidation residues in high-temperature oxidation zone under non-isothermal oxidation environment. After 425 °C isothermal pyrolysis, low temperature oxidation residue will produce more coke. Abdul Majidet al. [14] studied the characterization of two biomass pyrolysis oil samples by NMR spectroscopy using 1H and 13C NMR.

* Corresponding author. No.16, Li du Juxian Avenue, Fuling District, Chongqing, 408100, China.
*E-mail address:* 20180014@yznu.cn (J. Yuan).

https://doi.org/10.1016/j.jmgm.2019.05.013
1093-3263/

Semi-quantitative methods were used to evaluate the functional groups concerned in order to obtain the chemical structure information of the cracking oil. At present, there are few reports on the study of various structures, physical and chemical structures and dynamic characteristics of asphaltenes in oil-water interface by molecular dynamics simulation.

Finally, asphaltenes may be deposited in or near wellbore reservoirs, affecting oil recovery or separators and streamlines. The intervention cost of asphaltenes for offshore oil fields is about $500,000, the intervention cost for deep-water oil Wells is more than $500,000, the intervention cost for deep-water oil Wells is more than $1 million, and the intervention cost for deep-water oil Wells is more than $1 million. Some studies related to asphaltene aggregation have been carried out using experimental tools or mathematical model tools, which will greatly save costs [15–21]. Detailed molecular dynamics studies are needed to, understand the aggregation behavior of asphaltenes. Therefore, it is of great significance to understand the phase behavior of asphaltenes in oil production and refining, because asphaltenes have the potential to separate and aggregate with changes in crude oil temperature, pressure and composition [22,23]. The sedimentary mechanism and molecular structure are not completely clear. Care must be taken to understand the molecular underpinnings of asphaltene dynamics and their aggregation. Therefore, it is necessary to develop dynamic evaluation methods that can accurately simulate and predict the phase behavior of asphaltenes at the molecular scale.

## 2. Model and simulation methods

In order to study the asphaltene molecules within the scope of the phase behavior, we use the classic molecular dynamics (MD) simulation, MD simulation can depth study of oil-water interface structure parameters, the carbon in the bituminous asphalt chemical structure to find the change rule, reveal the influence mechanism of oil sands production, thus deepening understanding and awareness of the oil sands production process. This simulation mainly USES GROMACS 4.5.3 package [24,25] and GROMOS96 force field 24. The water molecules, dodecane molecules and asphalt molecules simulated in detail by MD are shown in Fig. 1 below. Among them, the complex structure and composition characteristics of the asphaltene molecular data were derived from the research results of Devon [26], and then the HYPERCHEM molecular modeling software [27] was used to create the 3D structure and optimize the geometry. Then the coordinates were exported and submitted to PRODRG to generate the topology file required by GROMACS molecular dynamic simulation [28]. The detailed molecular visualization of the system components is shown in Fig. 2 below. The red and gray atoms on either side or surrounded are water molecules, and the green molecules in the middle are dodecane molecules. There are two different initial interface models. The first one is composed of a 4.0 nm × 10.0 × 8.0 nm (x, y, and z) intermediate tank and two 2.0 nm × 8.0 × 8.0 nm water tanks on both sides (Fig. 2 (a)) and constructed using the molecular packaging program PACKMOL [29]. The initial simulation system was then placed in a large 12.0 nm × 12.0 nm simulation box. The water/oil interface simulation model is shown in Fig. 2 (b) below, which was built by genbox in GROMACS [24]. First, the molecular packaging program PACKMOL [29] creates an ordered array of 25 single types of bitumen molecules in a regular cube with an edge size of 8 nm. And then the box is filled with dodecane. Then the box expands in the x direction and is 12 nm long. The entire box is then randomly filled with water (Fig. 2(c), (d) and (e)). The oil phase consists of a series of n-alkanes called dodecane. We note that in all simulations, the number of dodecane and water molecules stabilized at 319 and 51815, respectively. Water and dodecane were used as the solvent for the simulation.

In MD simulation, in order to remove the initial strain in the system, the steepest descent method is used to minimize the energy of the initial configuration. Then, Langevin dynamics was used to balance the Maxwellian distribution at 300k in the NVT system with an initial velocity of 100ps, and MD simulation was started. In this simulation, periodic boundary conditions are applied on all three spatial dimensions, with the pressure and temperature of each system remaining constant. The oil phase of dodecane was described by the unified atomic model [34], and the aqueous phase was described by the SPC model. Explicit water/oil systems include water/dodecane, water/asphaltenes, and oil/asphaltenes. After the NVT setting as described above, the equilibrium operation of 100ps was carried out under the constant pressure of 1 atm (NPT) at 300k (coupling constant 0.01 ps), and then the MD operation of 5ns was carried out under the condition of 300k, which is the best efficient experiment condition [30]. In order to obtain good statistical data, we used LINCS algorithm to constrain the length of all c-h bonds and used a time step of 0.002 [31]. The temperature was controlled by hoover thermostat, and the relaxation time was 0.1ps [32–35]. In the specific MD simulation, the energy of the molecular system is described by simple potential energy functions, including bond stretching; bond Angle bending, tension, Lennard-Jones and electrostatic interactions. Only van der Waals interaction is used for bond stretching and bond Angle bending. In the GPL program, Visual Molecular Dynamics (VMD) is also used to visualize the trajectory and static images of the system. VMD is a molecular visualization program for the analysis of three-dimensional large

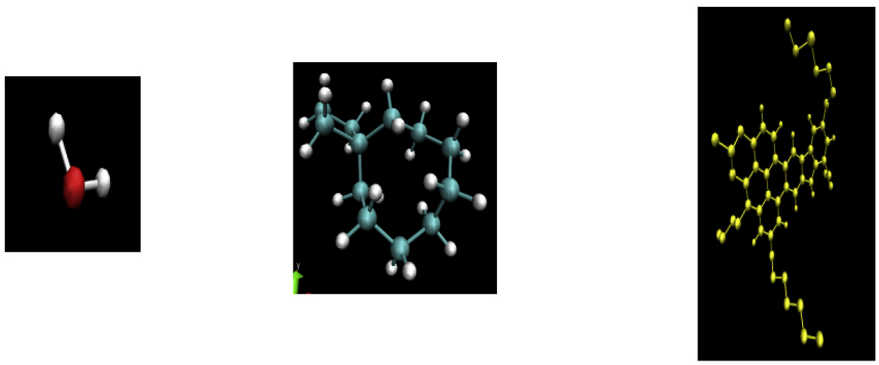

(a) Water: H2 O (b) Oil: dodecane (c) asphaltenes

**Fig. 1.** Molecules of the water, dodecane and asphaltenes.

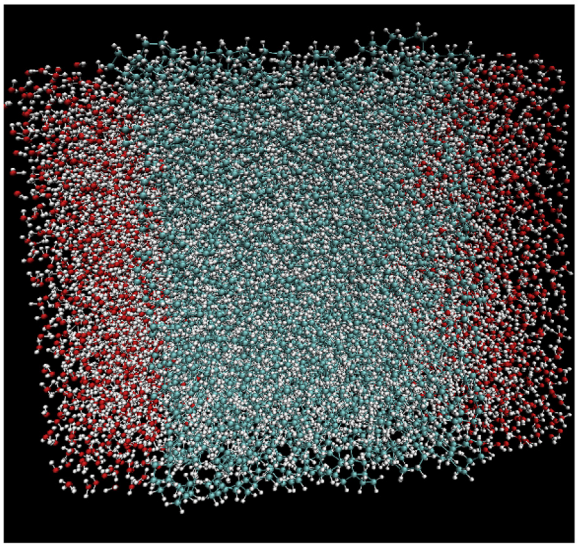

(a) water+oil+water

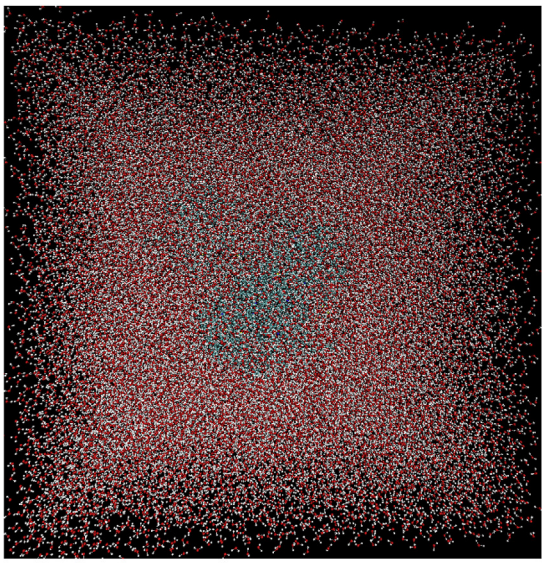

(b) oil surrounded by water

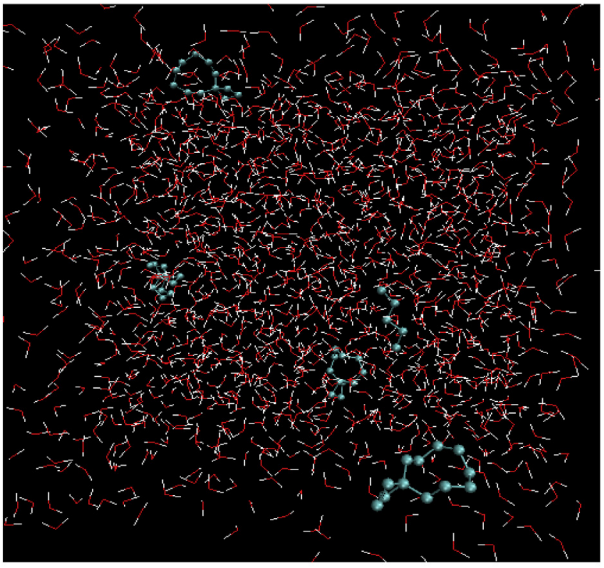

(c) begin of the system

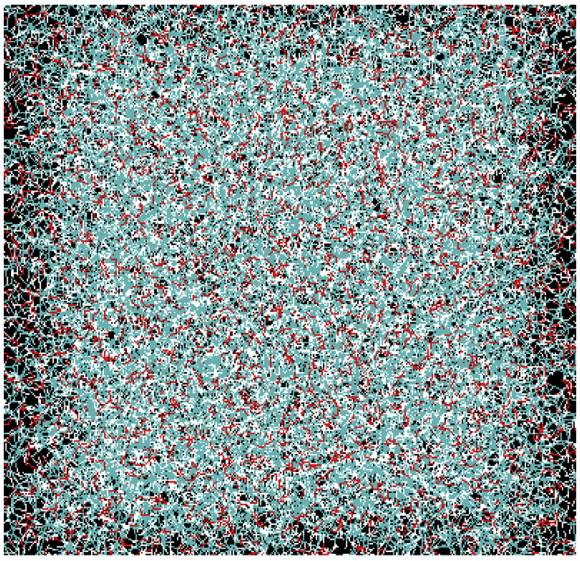

(d) system total mixed

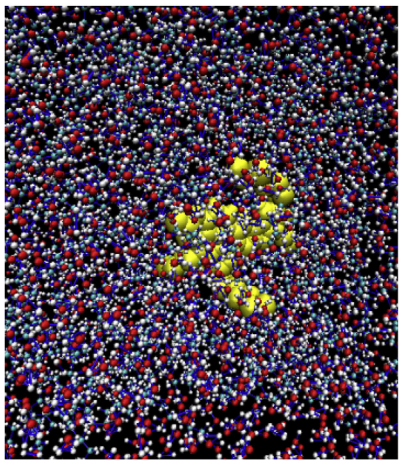

(e) system mixed shown asphaltenes

**Fig. 2.** The simulation model of the water/oil interface.

molecular systems developed by the University of Illinois at urbana-champaign [36]. It's designed to look at biological molecules, but it applies to all types of molecules; VMD is compatible with GROMACS format and can read configuration files and track files. In this visualization package, there are many ways to display molecules.

## 3. Results and discussion

Molecular dynamics simulation technology is feasible to analyze the chemical structure of tar sands asphaltenes, and a comprehensive and reasonable carbon structure framework has been established. Here are some detailed structural analysis results: density distribution profile, pair correlations (radial distribution function), root-mean-square deviation (RMSD), mean-square displacement (MSD) and diffusion coefficient.

### 3.1. Density distribution profiles

Fig. 3 shows the z-dependent density distribution of asphaltenes in the water/oil system. The density change is mainly caused by the different proportion of asphaltenes in the water/oil interface and the way of dissolution [37]. Generally, for a confined space, the adsorption energy of different molecules tends to affect the density distribution of each component. The number density distribution of methane mixed with different molecules, for example, water, carbon dioxide and nitrogen in nanotubes is discussed in Ref. [38]. For water/oil systems, the calculated average bulk densities of water and dodecane were 0.989 (0.997) g/cm$^3$ and 0.748 (0.749) g/cm$^3$, respectively. As a class of solubility, asphaltenes have solubility parameters (1.17−1.92 wt %) and average density of 1.12 g/cm$^3$ at room temperature. The system has two liquid phase areas at both ends of the tank, and the vacuum space between the liquid phase plates is greater than 30 Å. The calculated density is in good agreement with the corresponding experimental value.

In the area of the water/oil interface, the graph of these molecules shows that there is a peak density in the presence of oil, and the density increases in the system, with the highest density in the plate at about 1 nm. This is due to the presence of oxygen atoms in the lipid composition. The asphalt quality is guaranteed in the central area of the dodecane layer; the dodecane molecules are denser at the edges of the film. The increase in the box edge density is also due to the hydrophilic region, because the uncharged asphaltenes are reverently located in the center of the solvent, pushing the aromatic solvent to the interface edge [39].

### 3.2. Mean square displacement

Mean Square Displacement (MSD) is the average distance a molecule moves on [40]. Definition is the limiting slope of MSD (t), considering the linear regime with a sufficiently long time interval, its self-diffusion coefficient D is related to these two equations, ri(t)-ri(0) is the (vector) distance traveled by molecule i over some time interval of length t, d is the dimension of the space. The MSD of a substance usually represents its displacement in space over time. The dissolution process of organic solvent is the diffusion process of solvent molecules to the asphalt layer: solvent molecules first diffuse to the asphalt layer on the surface of oil sands. After the viscosity of the asphalt layer decreases, the oil layer is peeled off from the oil sands surface under the action of shear force. Different solvent molecules have different diffusion capacities. Equation (1) gives the specific calculation method of mean square shift, and the self-diffusion coefficient can be determined by using this Equation (2). As shown in Equation (2), the mean square displacement (MSD) of oil, water and asphaltene molecules is shown in Fig. 4. Fig. 4 shows the MSD with respect to the parameters content to the time. The diffusion constant D (Table 1) can be obtained from the slope of the mean square displacement (MSD) curve of particles versus time, and the apparent diffusion constant (D) of each component at the water/oil interface is given according to Equations (1) and (2) in Table 1. As can be seen from Table 1, the components of water have a higher diffusivity than other components. These values are consistent with diffusion constants from NMR measurements, which suggest values between $1 \times 10^{-10}$ and $4 \times 10^{-10}$ m$^2$/s depending on concentration [41].

$$MSD(t) = \Delta \vec{r}_i(t)^2 = (\vec{r}_i(t) - \vec{r}_i(0))^2 \quad (1)$$

$$\lim_{t \to \infty} MSD(t) = 6Dt \quad (2)$$

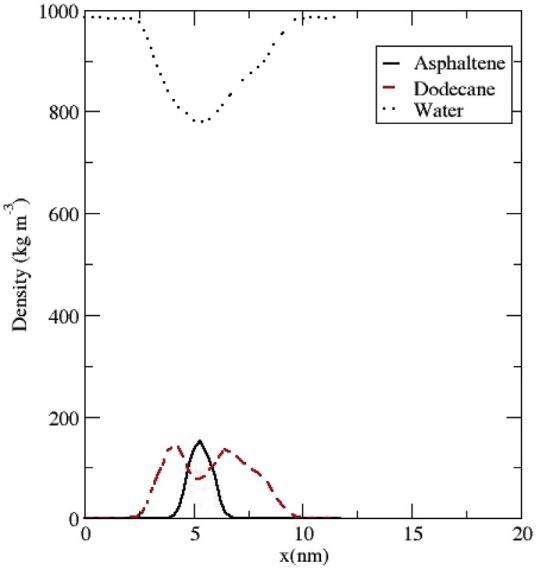


**Fig. 3.** Asphaltenes density profiles in the oil and water interfaces for the three parameters: oil, water, and Asphaltenes.

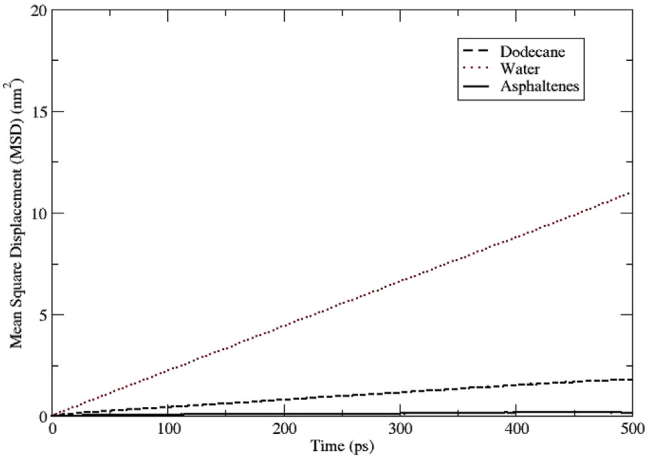


**Fig. 4.** Mean Square Displacement of the water, oil and asphaltene molecules in the water and oil interfaces.

**Table 1**
Diffusion constants (D) for three components in the water/oil interfaces.

| Diffusion coefficient | $\times 10^{-5}$ ($cm^2/s$) |
|---|---|
| Water | 3.6468 (±0.0347) |
| Oil | 0.8981 (±0.0255) |
| Asphaltene | 0.0531 (±0.00283) |

### 3.3. Radial distribution function

The radial distribution function gives the local density of species B around species A relative to the average density [42]. Fig. 5 shows the radial distribution function (RDFs) of different atomic groups of asphaltenes and water, asphaltenes and oil in polyaromatic rings. As shown in Fig. 5, the largest vertex (1.61 0.001) nanometer corresponds to a strong bond between the connecting polar head group of asphaltenes and oil molecules at the oil/water interface. Contrast, peak (5.922 + 0.001) nano asphaltene and between water molecules is far lower than the peak value as shown in Fig. 5, shows that the remote structure of the water phase, The main reason is that one hydrogen atom in some crude oil charge is larger than that in water, and the interaction between asphaltene magnetic head and crude oil asphalt magnetic head is stronger than that between head and water. At the same time, under the action of shear force, oil slurry on the surface of oil sands is spalling. Different solvent molecules have different diffusivity and dissolution rate. The mechanism of radial distribution function can better explain the dissolution phenomenon under the action of shear force. This result is consistent with the findings of Jian et al. [43] on the aggregation of asphaltenes in solvents (toluene) and water.

### 3.4. Root mean square deviation (RMSD)

Root mean square deviation (RMSD) is a measure of the average distance between atoms (usually main-chain atoms) [44] (Equation (3)). RMSD usually measures atomic correlation structures. As shown in Fig. 6, the matrix of atom positional root-mean-square deviations (RMSD) between pairs of structures was calculated for these sets of atoms: between asphaltene and water, between asphaltene and oil. The size of RMSD determines the degree of asphaltenes' movement in the water/oil interfaces. For small RMSD, the structural change of asphaltenes is not obvious, while for large RMSD, the structural change of asphaltenes is obvious.

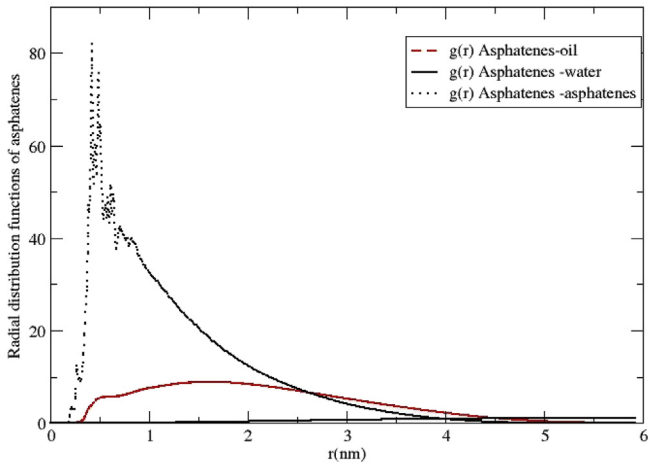


**Fig. 5.** Radial distribution function (RDF) of asphaltene in the water/oil interfaces as a function of time.

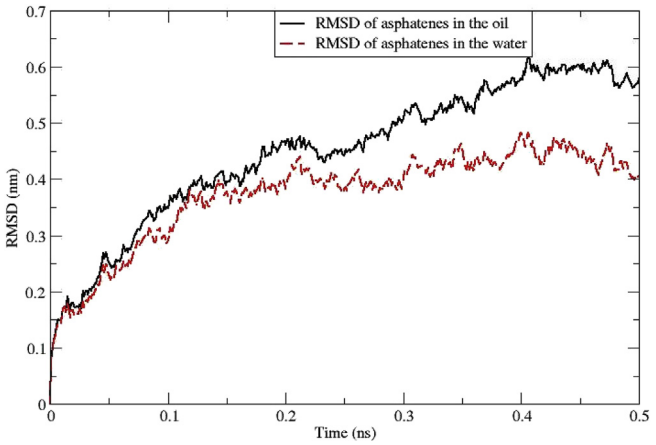


**Fig. 6.** Root-mean-square deviation (RMSD) of asphaltene in the water/oil interfaces as a function of time.

$$RMSD = \frac{1}{N}\left(\sum_{i}^{N}\sum_{j}^{N}\left(r_{ij}^{ref} - r_{ij}\right)^2\right)^{\frac{1}{2}} \quad (3)$$

As can be seen from Fig. 6, the RMSD value obtained is within a reasonable range. After the initial increase, the structural distance between asphaltenes and water fluctuates around 0.1 nm, indicating that the simulation is fully stable. The fluctuation distance between asphaltenes and crude oil is about 0.05 nm. The structural distance between asphaltenes and water changes more greatly than that between asphaltenes and oil [45].

### 3.5. Minimum distances

The minimum distance represents the minimum distance between two residues. The mean minimum distance matrix can be used to identify secondary and tertiary structures. According to Fig. 7, the average minimum distance between asphaltenes and oil

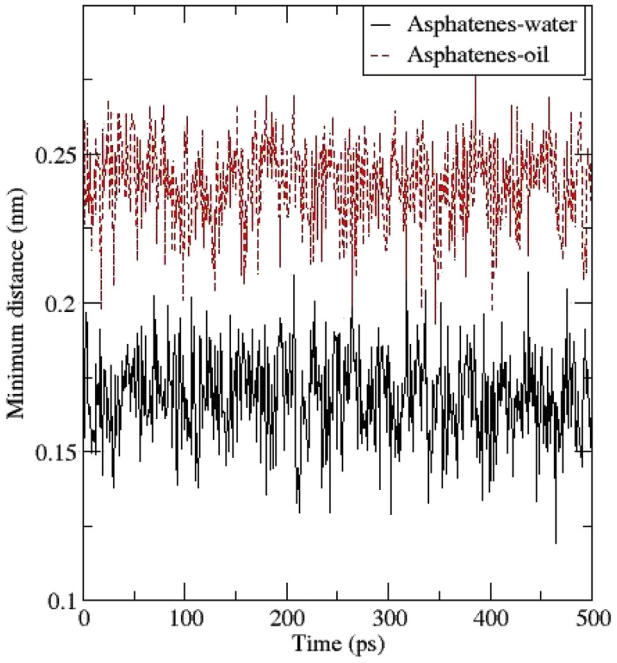


**Fig. 7.** Minimum distance of asphaltene in the water/oil interfaces as a function of time.

is 0.2375, and the average minimum distance between asphaltenes and water is 0.175, which is in good agreement with the findings of Pacheco-Sánchez et al. [46].

### 3.6. Radius of gyration

The calculation of the radius of gyration, Rg, gives a measure of the compactness of a cluster. As clusters become largely oblong in formation the radius of gyration is increased, where for spherical clusters the radius of gyration is representative of the cluster radius. Equation (4) shows how the square of the radius of gyration is calculated. M is the mass of particle i, and r is the radius to the center of mass. Therefore, Rg can take on values of x, y, and z.

$$r_{gyration} = \sqrt{\frac{\sum r^2 \cdot m}{\sum m}} \tag{4}$$

Simulation results reveal the diffusion behavior is excluded volume effect and the coupling of the fluid mechanics interaction as a result, in the process of diffusion, interaction of fluid mechanics to reduce rejection volume contribution to the diffusion behavior. As shown in Fig. 8, you can see that after 500 ps of MD simulation, radius of gyration also showed the trend of the asphaltene structures tend to be dense. For the corresponding values, Rg decreased from ~1.77681 Å to the mean value of $1.75 \pm 0.2$ Å for the asphaltene, whereas for the x direction, y direction, and z direction, the Rg mean values were $1.3 \pm 0.2$ Å, $1.27 \pm 0.2$ Å, and $1.68 \pm 0.1$ Å, respectively (Fig. 8). Therefore, MD simulation at a 500 ps radius of gyration shows that the elongation of the asphaltene chain conformation. Rg is lower in the x and y direction than it is in the z direction. This can be attributed to the relatively large electrostatic force in the z direction, which further inhibits the interaction between asphaltenes and smaller regions [47].

### 3.7. Rotational correlation functions

Correlation functions provide a measure of the disorder introduced into the system over time. Correlation functions can be thought of as memory functions that illustrate the need for time (delta t) in one variable (such as the dipole orientation) to lose Equation (5) with another variable (such as later the same dipole orientation). A correlation function with an object later is itself an autocorrelation function. A commonly used correlation function is the dot product of two vectors at different times, which indicates the correlation degree between two variables. The results show in Fig. 9 that the concentration decreases sharply with time. The larger the correlation, the more relevant it will be. The results are consistent with the study of Henning et al. who determined correlation degree using fluorescence depolarization techniques, addressing an active, long-standing controversy [48].

$$C(\tau) = u(t) \cdot v(t+\tau) \tag{5}$$

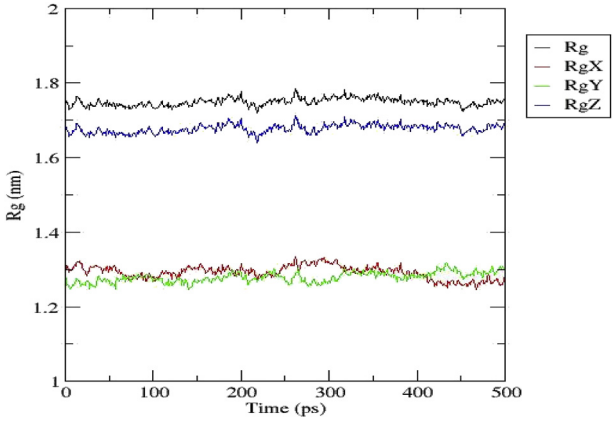


**Fig. 8.** Radius of gyration (Rg) for backbone heavy atoms of the asphaltene during 500 ps MD simulations.

### 3.8. Bulk viscosity

Bulk viscosity was obtained in the present study by the direct application of Green-Kubo equation [40].

$$\eta^V = \frac{V}{K_B T} \int_0^\infty dt(\delta P(t)\delta P(0) \tag{6}$$

V is the volume of the simulated cells, $\boldsymbol{K_B}$ is Boltzmann constant, **T** is absolute temperature and $\boldsymbol{\delta P(t)}$=$\boldsymbol{P(t)}$− <$\boldsymbol{P(t)}$> with $\boldsymbol{P(t)}$ as instantaneous pressure simulation system at time T and <P(t)> as the average pressure on the whole simulation time. The instantaneous pressure P (t) is obtained by averaging the three diagonal elements of the stress tensor. δP (t) δ P (0) represents an auto-correlation function of δP and was referred to hereafter as bulk auto-correlation function. Therefore, the calculation of volume viscosity mainly involves the integral of volume auto-correlation function. The viscosity results are shown in Fig. 10. The volume viscosity is approximately $10^{-3}$ pa s, and the excess volume viscosity in the mixture will fluctuate. In Fig. 10, two typical peaks occur at 50ps and 180ps, respectively. Basically, the volume viscosity of the molecular is determined by molecular simulations for two main reasons: the contribution of the dilute gas generated by the relaxation of internal degrees of freedom and the contribution of the configurations generated by the molecular interactions [49].

### 3.9. Free energy analysis

**ΔG** sign tell us in which direction to reach equilibrium reaction. ΔG tells us how far the size of the reaction is balance now. The free energy can be defined as the free energy difference given by the total reversible work when the Hamiltonian of the system changes from gas to liquid [50]. Free energy ΔG estimated using thermodynamics integral method [51,52] algorithm is as follows Equation (7). For λ value, the equation is a coupling parameter and the λ value is usually between 0 and 1, and the equilibrium average can be used to evaluate the free energy of derivatives to λ. λ is the completely interacting solute, with no relation to $\lambda = 1$. To calculate the free energy, several independent simulations of asphaltenes in solvents with different coupling parameters (oil and water) are required. The emulation is repeated with the following 6 λ values:(0, 0.2, 0.4, 0.6, 0.8, and 1).

$$\Delta G = \int_0^1 \frac{\partial G(\lambda)}{\partial \lambda} d\lambda \tag{7}$$

The free energy difference of asphaltenes is shown in Table 2. The free energy difference of water phase is obviously smaller than that of oil phase. In Table 2, Gromacs is also used to calculate the comprehensive free energy of asphalt quality pairs in more detail. They found an asphaltene with a total free energy of 417.12−1866.16 kJ/mol in the oil phase and 472.83−1784.17 kJ/mol in the water phase. The results of Figs. 11 and 12 show that the asphaltenes and solvents (water and oil) molecules obtain higher

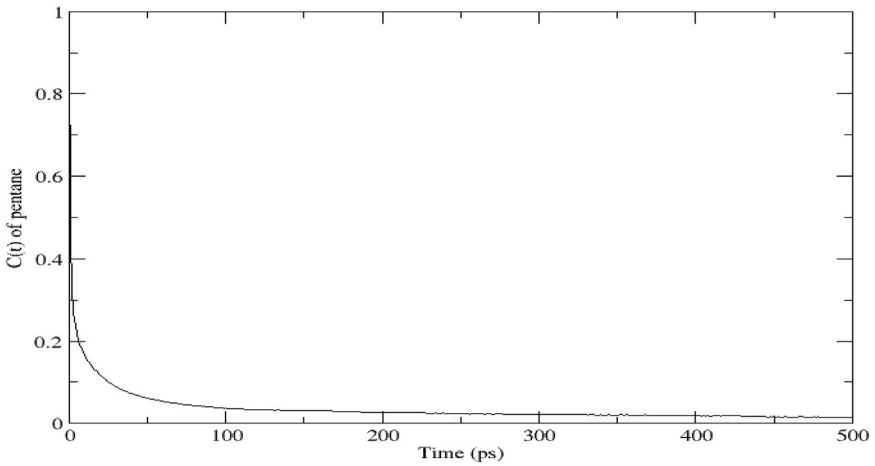


**Fig. 9.** Rotational correlation function of asphaltene in the water/oil interfaces.

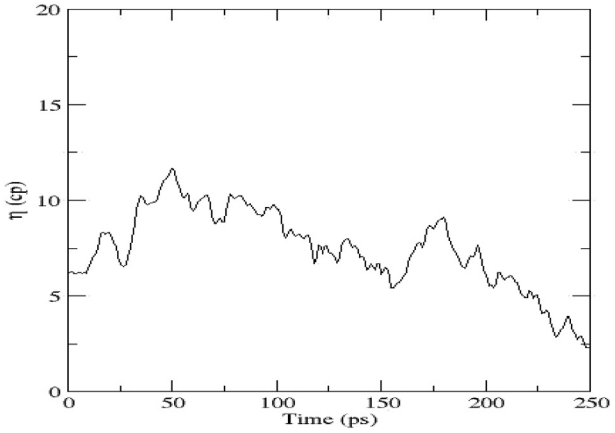


**Fig. 10.** Bulk viscosity of asphaltene in the water/oil interfaces.

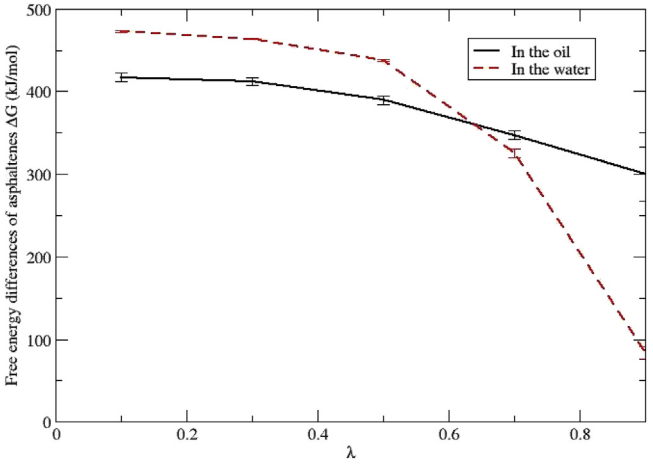


**Fig. 11.** Free energy differences of asphaltenes as a function of $\lambda$ using the Gromacs.

**Table 2**
Free energy difference and integrated energy of asphaltene in the water and oil phases.

| $\lambda$ values | In the oil phase (kJ/mol) | | | In the water phase(kJ/mol) | | |
|---|---|---|---|---|---|---|
| | Integrated energy | Free energy difference | | Integrated energy | Free energy difference | |
| 0.2 | 417.12 | 417.12 | 5.24 | 472.83 | 472.83 | 0.93 |
| 0.4 | 829.23 | 412.11 | 4.35 | 936.83 | 464.00 | 0.48 |
| 0.6 | 1219.09 | 389.86 | 5.37 | 1374.69 | 437.86 | 0.92 |
| 0.8 | 1566.43 | 347.34 | 4.89 | 1700.05 | 325.35 | 5.37 |
| 1.0 | 1866.16 | 299.73 | 32.7 | 1784.17 | 84.12 | 7.44 |

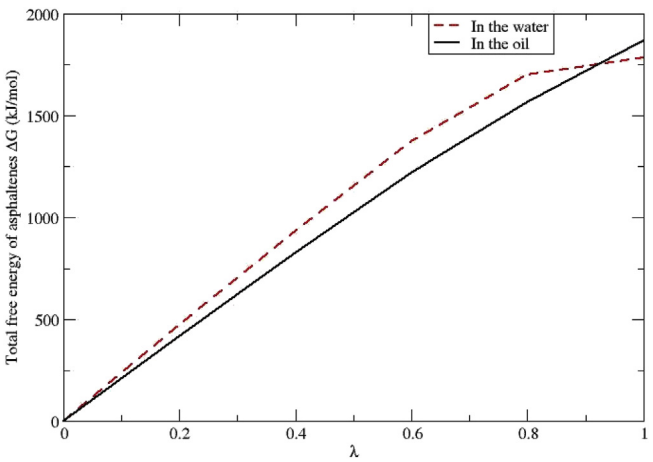


**Fig. 12.** Total free energy differences of asphaltenes as a function of $\lambda$ using the Gromacs.

thermal free energy, making the molecules more fluid and easier to break the bonds between molecules [53].

## 4. Discussions

In recent years, MD simulation technology has been widely and successfully applied in the field of petroleum and natural gas system [54]. Understanding the molecular interactions between asphaltenes and other molecules will contribute to a better understanding of their stability in petroleum fluids and their phase transition properties. Before application, it is very important to understand the molecular level of the factors affecting the interface force of asphaltene-solvent-water. The results of root mean square deviation (RMSD), radius of gyration, minimum distance, concentration correlation function and volume viscosity showed that the detailed dynamic characteristics of asphaltenes at the water/oil interface position and monocular distance varied with the

simulation time [45–49]. Methylene carbon is the main contribution of oil production, and the average length of aliphatic chain is constantly shortened. As the temperature increases, aliphatic carbon loss will be more serious. Finally, the free energy of the asphaltenes, the total free energy will increase with the increase of lambda means that the asphaltenes molecules are more easily moved and can destroy the association of molecules [53]. The MD simulation results of asphaltenes at the oil-water interface show that the solubility of oil and water affects the asphaltenes at the oil-water interface, so that the asphaltenes have different ability to flow and destroy molecular association, indicating that the structure and dynamic performance of asphaltenes are different at the oil-water interface and water-water interface. The simulation results show that asphaltenes tend to form aggregates above the critical concentration, which is like the asphaltene nanoaggregates reported in earlier literature [1,6,17,and 1]. And then the simulation results of the diffusion of asphaltic oil/water interface, and the diffusion of pure asphalt, it is by vacuum degree of vacuum $m^2/s$. $0.5 \times 1.4\ m^2/s$ show lateral diffusion of the dominance of asphaltene seems to imitate the lipid encountered in oil/water interfacial diffusion characteristics, however, in the pure toluene, diffusion will be about $1.2 \times$ vacuum $m^2/s$, it proved the correctness of the result, asphaltene can't dissolve in the water/oil interface, can only be dissolved in toluene [56]. However, the difference in free energy with λ increases will decrease. By means of molecular dynamics simulation, more information about the atomic scale structure and dynamic properties of different solvent systems can be obtained.

## 5. Conclusions

In this paper, it is feasible to analyze the chemical structure of tar sands asphaltenes by molecular dynamics simulation technique, which can not only comprehensively and reasonably analyze the carbon structure skeleton, but also accurately and credibly analyze the results. Simulation shows the oil/water interface asphaltene molecular structure and dynamics calculation results, the density profile, the radial distribution function, root mean square deviation (RMSD), root mean square displacement (MSD), diffusion coefficient, turning radius, minimum distance and the concentration of the correlation function and the bulk viscosity of asphaltene molecules was discussed from the aspects such as structure and dynamic behavior. Results also points out that the asphaltenes in the structure and dynamics properties of oil and water interface is different, the oil sands separation in the main consideration is to reduce the interfacial tension, the emulsification and flows, wettability change and rigidity interface membrane, the principle of the asphalt from the oil-water interface aggregation and distribution mutual tension and emulsification in oil-water interface interaction between density distribution and the partition of the asphaltenes, especially hydrogen bonding on the oil-water interface is likely to be affected aggregate shape, position and orientation of the most important interactions. In addition, asphaltenes are mainly associated with water and aromatic bitumen. The hydro-asphaltene interaction leads to the formation of emulsion, and the aromatic-clay interaction leads to clay migration and the increase of asphaltene precipitation.

## Acknowledgement

This study was partially supported by a Discovery Research Grant from Yangtze Normal University (Fund No. FLKJ,2018BBB3017) and Canada ecoEII Clean Energy Funds.

## References

[1] S.S. Betancourt, G.T. Ventura, A.E. Pomerantz, O. Viloria, F.X. Dubost, J. Zuo, G. Monson, D. Bustamante, J.M. Purcell, R.K. Nelson, R.P. Rodgers, Nanoaggregates of asphaltenes in a reservoir crude oil and reservoir connectivity, Energy Fuels 23 (3) (2008 Dec 19) 1178–1188.
[2] X.H. Wang, X.F. Huang, K. Lin, Y.P. Zhao, The constructions and pyrolysis of 3D kerogen macromolecular models: experiments and simulations, Glob. Chall. 3 (2019) 1900006.
[3] M. Fossen, H. Kallevik, K.D. Knudsen, J. Sjöblom, Asphaltenes precipitated by a two-step precipitation procedure. 2. Physical and chemical characteristics, Energy Fuels 25 (8) (2011 Aug 2) 3552–3567.
[4] K.L. Gawrys, P. Matthew Spiecker, P.K. Kilpatrick, The role of asphaltene solubility and chemical composition on asphaltene aggregation, Petrol. Sci. Technol. 21 (3–4) (2003 Jan 5) 461–489.
[5] K.L. Gawrys, P.K. Kilpatrick, Asphaltene aggregation: techniques for analysis, Instrum. Sci. Technol. 32 (3) (2004 Dec 27) 247–253.
[6] T.F. Headen, E.S. Boek, N.T. Skipper, Evidence for asphaltene nanoaggregation in toluene and heptane from molecular dynamics simulations, Energy Fuels 23 (3) (2009 Feb 2) 1220–1229.
[7] S. Acevedo, B. Borges, F. Quintero, V. Piscitelly, L.B. Gutierrez, Asphaltenes and other natural surfactants from Cerro Negro crude oil. Stepwise adsorption at the water/toluene interface: film formation and hydrophobic effects, Energy Fuels 19 (5) (2005 Sep 21) 1948–1953.
[8] T. Dabros, Interparticle hydrodynamic interactions in deposition processes, Colloids Surface. 39 (1–3) (1989) 127–141.
[9] T. Dabros, T.G. Van De Ven, Collision-induced dispersion of droplets attached to solid particles, J. Colloid Interface Sci. 163 (1) (1994 Mar 1) 28–36.
[10] Y. Fan, S. Simon, J. Sjöblom, Interfacial shear rheology of asphaltenes at oil–water interface and its relation to emulsion stability: influence of concentration, solvent aromaticity and nonionic surfactant, Colloid. Surf. Physicochem. Eng. Asp. 366 (1–3) (2010 Aug 20) 120–128.
[11] Park Young Cheol, Paek Jin-Young, Bae Dal-Hee, et al., Study of pyrolysis kinetics of Alberta oil sand by thermogravimetric analysis, Korean J. Chem. Eng. 26 (6) (2009) 1608–1612.
[12] Pulikesi Murugan, Nader Mahinpey, Thilakavathi Mani, et al., Effect of low-temperature oxidation on the pyrolysis and combustion of whole oil, Energy 35 (5) (2010) 2317–2322.
[13] Abdul Majid, Indu Pihillagawa, Potential of NMR spectroscopy in the characterization of nonconventional oils, J. Fuels 2014 (1) (2014) 1–7.
[14] S. Acevedo, M. Caetano, M.A. Ranaudo, B. Jaimes, Simulation of asphaltene aggregation and related properties using an equilibrium-based mathematical model, Energy Fuels 25 (8) (2011 Aug 2) 3544–3551.
[15] N. Aske, H. Kallevik, E.E. Johnsen, J. Sjöblom, Asphaltene aggregation from crude oils and model systems studied by high-pressure NIR spectroscopy, Energy Fuels 16 (5) (2002 Sep 18) 1287–1295.
[16] I.N. Evdokimov, Characterization of asphaltenes and crude oils by near-UV/visible absorption spectroscopy, Asphaltenes: Charac. Prop. Appl. (2010) 1–46.
[17] J. Eyssautier, P. Levitz, D. Espinat, J. Jestin, J. Gummel, I. Grillo, L. Barré, Insight into asphaltene nanoaggregate structure inferred by small angle neutron and X-ray scattering, J. Phys. Chem. B 115 (21) (2011 May 10) 6827–6837.
[18] S. Goncalves, J. Castillo, A. Fernandez, J. Hung, Absorbance and fluorescence spectroscopy on the aggregation behavior of asphaltene–toluene solutions, Fuel 83 (13) (2004 Sep 1) 1823–1828.
[19] S.G. Abreu, J.A. Castillo, A. Fernandez, S. Acevedo, Evidence of molecular aggregation of asphaltenes by using induced laser fluorescence technique, in: In19th Congress of the International Commission for Optics: Optics for the Quality of Life, vol 4829, 2003 Nov 19, pp. 829–831 (International Society for Optics and Photonics).
[20] L. Goual, M. Sedghi, H. Zeng, F. Mostowfi, R. McFarlane, O.C. Mullins, On the formation and properties of asphaltene nanoaggregates and clusters by DC-conductivity and centrifugation, Fuel 90 (7) (2011 Jul 1) 2480–2490.
[21] M.R. Gray, R.R. Tykwinski, J.M. Stryker, X. Tan, Supramolecular assembly model for aggregation of petroleum asphaltenes, Energy Fuels 25 (7) (2011 Jul 1) 3125–3134.
[22] S.I. Andersen, E.I. Stenby, Thermodynamics of asphaltene precipitation and dissolution investigation of temperature and solvent effects, Fuel Sci. Technol. Int. 14 (1–2) (1996 Jan 1) 261–287.
[23] C.W. Angle, Y. Long, H. Hamza, L. Lue, Precipitation of asphaltenes from solvent-diluted heavy oil and thermodynamic properties of solvent-diluted heavy oil solutions, Fuel 85 (4) (2006 Mar 1) 492–506.
[24] Gromacs Manual. http://www.gromacs.org/Downloads.
[25] H.J. Berendsen, D. van der Spoel, R. van Drunen, GROMACS: a message-passing parallel molecular dynamics implementation, Comput. Phys. Commun. 91 (1–3) (1995 Sep 2) 43–56.
[26] Y. Xu, T. Dabros, H. Hamza, W. Shefantook, Destabilization of water in bitumen emulsion by washing with water, Petrol. Sci. Technol. 17 (9–10) (1999 Oct 1) 1051–1070.
[27] Hyper Manual. www.hyper.com/.
[28] A.W. SchuÈttelkopf, D.M. Van Aalten, PRODRG: a tool for high-throughput crystallography of protein–ligand complexes, Acta Crystallogr. Sect. D Biol. Crystallogr. 60 (8) (2004 Aug 1) 1355–1363.
[29] J.M. Martínez, L. Martínez, Packing optimization for automated generation of

complex system's initial configurations for molecular dynamics and docking, J. Comput. Chem. 24 (7) (2003 May 1) 819–825.
[30] G.S. Anderson, R.C. Miller, A.R. Goodwin, Static dielectric constants for liquid water from 300 K to 350 K at pressures to 13 MPa using a new radio-frequency resonator, J. Chem. Eng. Data 45 (2000) 549–554.
[31] B. Hess, H. Bekker, H.J. Berendsen, J.G. Fraaije, LINCS: a linear constraint solver for molecular simulations, J. Comput. Chem. 18 (12) (1997 Sep 1) 1463–1472.
[32] S. Nosé, M.L. Klein, A study of solid and liquid carbon tetrafluoride using the constant pressure molecular dynamics technique, J. Chem. Phys. 78 (11) (1983 Jun 1) 6928–6939.
[33] S. Nosé, A unified formulation of the constant temperature molecular dynamics methods, J. Chem. Phys. 81 (1) (1984 Jul 1) 511–519.
[34] A. Kukol, Lipid models for united-atom molecular dynamics simulations of proteins, J. Chem. Theory Comput. 5 (3) (2009 Feb 20) 615–626.
[35] H.J. Berendsen, J.P. Postma, W.F. van Gunsteren, J. Hermans, Interaction models for water in relation to protein hydration, InIntermolecular forces (1981) 331–342 (Springer).
[36] W. NetherlandsHumphrey, A. Dalke, K. Schulten, VMD: visual molecular dynamics, J. Mol. Graph. 14 (1) (1996 Feb 1) 33–38.
[37] M.S. Diallo, T. Cagin, J.L. Faulon, W.A. Goddard Iii, Thermodynamic properties of asphaltenes: a predictive approach based on computer assisted structure elucidation and atomistic simulations, in: Developments in Petroleum Science, vol 40, Elsevier, 2000 Jan 1, pp. 103–127.
[38] K. Lin, Q. Yuan, Y.P. Zhao, C.M. Cheng, Which is the most efficient candidate for the recovery of confined methane: water, carbon dioxide or nitrogen? Extr. Mech. Lett. 9 (2016) 127–138.
[39] P.M. Spiecker, K.L. Gawrys, P.K. Kilpatrick, Aggregation and solubility behavior of asphaltenes and their subfractions, J. Colloid Interface Sci. 267 (1) (2003 Nov 1) 178–193.
[40] C.R. Iacovella, A.S. Keys, S.C. Glotzer, Self-assembly of soft-matter quasicrystals and their approximants, Proc. Natl. Acad. Sci. Unit. States Am. 108 (52) (2011 Dec 27) 20935–20940.
[41] N.V. Lisitza, D.E. Freed, P.N. Sen, et al., Study of asphaltene nanoaggregation by nuclear magnetic resonance, Energy Fuels 23 (2009) 1189–1193.
[42] E. Matteoli, G.A. Mansoori, A simple expression for radial distribution functions of pure fluids and mixtures, J. Chem. Phys. 103 (11) (1995 Sep 15) 4672–4677.
[43] C. Jian, T. Tang, S. Bhattacharjee, Molecular dynamics investigation on the aggregation of Violanthrone78-based model asphaltenes in toluene, Energy Fuels 28 (2014) 3604–3613.
[44] S.B. Dixit, S.Y. Ponomarev, D.L. Beveridge, Root mean square deviation probability analysis of molecular dynamics trajectories on DNA, J. Chem. Inf. Model. 46 (3) (2006 May 22) 1084–1093.
[45] W.G. Hoover, D.J. Evans, R.B. Hickman, A.J. Ladd, W.T. Ashurst, B. Moran, Lennard-Jones triple-point bulk and shear viscosities. Green-Kubo theory, Hamiltonian mechanics, and nonequilibrium molecular dynamics, Phys. Rev. 22 (4) (1980 Oct 1) 1690–1697.
[46] J.H. Pacheco-Sánchez, R. Alejo, H. Cruz-Reyes, F. Álvarez-Ramírez, Neural networks to fit potential energy curves from asphaltene-asphaltene interaction data, Fuel 236 (2019) 1117–1127. https://doi.org/10.1016/j.fuel.2018.09.031, 0016–2361.
[47] Joëlle Eyssautier, Didier Frot, Loïc Barré, Structure and dynamic properties of colloidal asphaltene aggregates, Langmuir 28 (33) (2012) 11997–12004, https://doi.org/10.1021/la301707h.
[48] Henning Groenzin, C. Oliver, Mullins, Asphaltene molecular size and structure, J. Phys. Chem. A 103 (50) (1999) 11237–11245, https://doi.org/10.1021/jp992609w.
[49] Frederike Jaeger, Omar Matar, Erich Müller, Bulk viscosity of molecular fluids, J. Chem. Phys. 148 (2018) 174504.
[50] P. Kollman, Free energy calculations: applications to chemical and biochemical phenomena, Chem. Rev. 93 (7) (1993 Nov 1) 2395–2417.
[51] M. Sprik, G. Ciccotti, Free energy from constrained molecular dynamics, J. Chem. Phys. 109 (18) (1998 Nov 8) 7737–7744.
[52] T. Maqbool, S. Raha, M.P. Hoepfner, H.S. Fogler, Modeling the aggregation of asphaltene nanoaggregates in crude oil– precipitant systems, Energy Fuels 25 (4) (2011 Mar 7) 1585–1596.
[53] J.S. Chickos, J.R. Acree, Enthalpies of vaporization of organic and organometallic compounds, J. Phys. Chem. Ref. Data 32 (2003) 519–878.
[54] James A. Platts, J. Grant Hill, Non-covalent interactions using local correlation methods: energy partitioning, geometry optimisation and harmonic frequency calculations, Mol. Phys. 108 (11) (2010) 1497–1504, https://doi.org/10.1080/00268971003757977.
[55] E.M. Freer, C.J. Radke, Relaxation of asphaltenes at the toluene/water interface: diffusion exchange and surface rearrangement, J. Adhes. 80 (6) (2004 Jun 1) 481–496.
[56] K. Norinaga, V.J. Wargardalam, S. Takasugi, M. Iino, S. Matsukawa, Measurement of self-diffusion coefficient of asphaltene in pyridine by pulsed field gradient Spin– echo 1H NMR, Energy Fuels 15 (5) (2001 Sep 19) 1317–1318.